



Experimental and Numerical Analysis of Air Gap Insulation for Thermal Performance Enhancement in Polyethylene Water Storage Tanks

Jaafar Ali Mahdi^{ID}, Hasanain J.A. Juaifer^{*ID}, Ali A. Abdulrasool^{ID}

Mechanical Engineering Department, College of Engineering, University of Kerbala, Karbala 56001, Iraq

Corresponding Author Email: hassanen.j@uokerbala.edu.iq

Copyright: ©2025 The authors. This article is published by IIETA and is licensed under the CC BY 4.0 license (<http://creativecommons.org/licenses/by/4.0/>).

<https://doi.org/10.18280/ijht.430207>

ABSTRACT

Received: 10 February 2025

Revised: 26 March 2025

Accepted: 9 April 2025

Available online: 30 April 2025

Keywords:

water tank insulation, cooling and heating, experimental study, numerical simulation

Hot and cold water from household tanks can cause significant issues for residential and agricultural buildings in the Middle East, particularly in Iraq, where temperatures can reach 50°C in summer and -5°C in winter. Numerous methods and procedures were used to lower or enhance tank output water temperature, but their efficiency varied. In this study, numerical and experimental tests were used to find out how different practices (air gap) affect the thermal performance of the water tanks. The goal was to find the best practice that could be used to protect the water inside the tanks from the harsh outside environment (like sunlight intensity and air temperature). To limit the amount of heat that was transferred from or to the tank, two tanks of the same size and color were utilized. The first tank did not have an air gap, while the other tank was surrounded by an air gap. A comparison is made between the findings obtained from the theoretical prediction of water tanks and the data obtained from their experiments. The findings indicated that the air gap lowers heat transfer rate by about 10% during summer and 8% during winter.

1. INTRODUCTION

Iraq has a hot, dry climate with long, hot, dry summers that can get as hot as 55°C and short, cool winters that can get as cold as -8°C. Iraq is situated between the subtropical dryness of the Arabian deserts and the subtropical wetness of the Gulf, which affects the weather.

As long as humans have been civilized, there has been a need for water tanks to store water for human consumption, plant irrigation, fire prevention, drinking water for poultry and livestock, manufacturing chemicals, food preparation, and many other uses.

In Iraq, people store water in tanks that they put on the roofs of their homes so that the water has the right amount of hydraulic pressure. This kind of behavior was also seen in industrial and agricultural operations. The general design of a water tank and the materials used to construct it are important considerations. The most common materials used to make water tanks are steel (either carbon or stainless steel), fiberglass, concrete, stone, and plastics (polyethylene and polypropylene).

During the summer and winter, hot and cold water from water tanks is a big problem, especially in residential buildings in Iraq, where water temperatures can reach over 50°C in the summer and below -5°C in the winter. To avoid this, people work hard to keep water tanks from getting heated by the sun or the air around them. There were ways and habits that were used to cool down the water that came from home pools.

Numerous studies have found that the appliances used to provide hot or cold water consume some of household energy [1-3].

Rodriguez et al. [4] investigated the transient cooling of a fluid initially at rest within a vertical cylinder, experiencing heat loss through its walls. They claimed that the proposed link between the global thermodynamic model and the Nusselt number can both anticipate the transient behavior of the fluid temperature inside the tank and quantify heat losses to the environment. Fan and Furbo [5] conducted research on the thermal stratification that occurs in a hot water tank as a result of heat loss, taking into consideration the ratio of the tank's volume to its diameter, the insulation of the tank, and the initial conditions of the tank. Their findings indicated that 20–55% of the lateral heat loss is transferred to the underlying layers when the temperature gradient ranges from 0.2 to 1.5 K/m, suggesting that heat loss from the tank contributes to the establishment of thermal stratification within the tank. Oliveski [6] The short-term cooling process in a cylindrical vessel that stands vertically was numerically analyzed to establish a correlation between the internal heat transfer rate and the primary factors that regulate the cooling process. An improved thermal water storage tank with increased energy storage capacity was developed by Armstrong et al. [7] using a combination of copper, stainless steel, and rigid, cross-linked polyurethane as insulation. This study's findings indicate that stainless steel is a superior alternative to copper due to its enhanced thermal performance, cost-effectiveness, and superior tensile strength compared to copper. Utilising polyethylene would lead to a diminished rate of destratification compared to stainless steel; nevertheless, polyethylene is associated with increased biofilm proliferation and would require supplementary materials to offset its inadequate tensile strength.

Padovan et al. [8] created a novel model for ESP-r that simulates a tank-in-tank thermal storage system. The tank-in-tank device has two tanks. The smaller tank holds hot water that can be drunk. The bigger buffer is full of water for the heating circuit. The model results matched the experimental results pretty well, and it can correctly show how the water flows in the external tank during the discharge time. Yang et al. [9] looked at how the shape of a water tank affects its ability to store heat and its thermal stratification. It was shown that a cylinder with acute angles exhibits the highest degree of thermal stratification, whilst those with a flat, horizontal surface demonstrate the least. Avignon and Kummert [10] used a dynamic test bench to look at how well the phase change material (PCM) storage tank worked in a range of different working conditions.

Cruikshank and Harrison [11] used both computational and experimental methods to study the efficiency of SDHW systems. They found that the tank's bottom accounted for a sizable portion of the heat lost to the surroundings. Additionally, Abdelhak et al. [12] examined the flow properties and evolution of thermal stratification in a hot water storage vessel during charging and discharging using a three-dimensional computational fluid dynamics (CFD) model. Their research showed that, when it came to stratified storage tanks, the vertical orientation design was superior to the horizontal one. A model shown by Rahman et al. [13] depicts a pressurised water tank equipped with two heat exchangers, one for hot water and one for cold water. The model employed one-dimensional, transient heat balance formulae to determine the temperature profiles at a specific height. Additionally, they investigated the impact of heat sources, flow rates, and the location and length of the heat exchangers on the buoyancy of the tank. The findings indicated that the temperature of the water that is retained and the cold water that exits the heated heat exchanger increases as the flow rate increases. Erdemir et al. [14] showed an experimental study that investigated the impact of obstacles on the thermal performance of a horizontal mantled hot water tank. They discovered that adding obstacles to a horizontally supported hot water tank made it work better at keeping heat in. The temperature distribution results indicated that the temperature and quantity of heated water stored increased as a result of the introduction of an obstacle within the tank.

In order to determine which insulation geometries were most efficient in producing thermal stratification in both rectangular and cylindrical hot water tanks, Kursun [15] conducted research. According to the findings, the most effective tank shapes were truncated cone and pyramid.

Furthermore, Kursun and Okten [16] investigated the effects of corner ratio and positioning on the enhancement of thermal stratification in a rectangular hot water tank. They discovered that the exergy loss was barely affected by the shift in the tank's orientation and aspect ratio. Additionally, the tank's heat storage capacity was diminished due to the reduction in its aspect ratio. Bouzaher et al. [17] developed a computational model for a new type of storage tank that takes advantage of height stratification by studying the heat stratification in a circular water tank. A larger temperature differential existed between the water layers in the tank containing the case made of hollowed-out wood blocker compared to the other cases. Bai et al. [18] explored, both experimentally and computationally, the impact of water pit geometry on thermal capacity, stratifications, and performance, as well as the effects of height and side wall slope. It turns out

that as time goes on, a water pit's yearly storage efficiency goes up, its yearly heat loss goes down, and the soil surrounding the pit gets hotter. Janakarajan et al. [19] developed an insulated tank capacity 29 liters and analyzed energy storage performance numerically with silica gel and polyurethane attached to concrete tank. They employed the response surface method and grey relation analysis to optimise the results. Khoury et al. [20] developed an optimisation process taking into account tank size and design parameter constraints for the Thermal Energy Storage (TES) tank combined with Phase Change Materials (PCMs) for domestic water heating applications. Considering different control strategies for the multiple entrance independent phase change material modules and the traditional cascaded system, they outlined the ideal design parameters for two different thermal energy storage configurations.

Hwang et al. [21] compared new building materials to traditional ones for thermal insulation. The research approach improved paper-based cellulose insulation by adding porous aerogel powders. They employed a mixed control group that had 30 weight percent ceramic binder and 40 weight percent expandable graphite, as well as a pure control group that was packaged entirely of recycled cardboard. In the pure control and experimental groups, aerogel improved thermal insulation performance by 16.66%, whereas in the combined control and experimental groups, it improved performance by 17.06%. Liu et al. [22] suggested a new water storage tank to improve geothermal energy use in a system that combines geothermal heating with energy storage. A horizontally orientated multi-slot form with a flow equalising plate in the center made up the tank's structure. To assess the performance of the water storage tank, they created an experimental setup. According to the results, the new tank showed a thermocline thickness relation to tank height, ranging from 20.25 to 33.75%, which was less than that of a conventional water storage tank under the same operating conditions.

When looking through the published research on this subject, it is clear that the studies that have been carried out have investigated the effects of several parameters, including the kind of insulating materials used, the design of the tank, the capacity of the tank, and the utilization of PCMs for heat storage. Moreover, there are numerous studies that have been published in the academic literature that have utilized various insulating materials at the optimal thickness on the walls of buildings. As a result, the purpose of this study is to build an insulation tank that has a low cost and energy loss in the Iraqi environment by making use of air gap.

2. ANALYSIS OF ERROR IN TEMPERATURE MEASUREMENT

An uncertainty analysis is required to verify the error of temperature measurement in the experiment bench. If R is a linear function of i independent variables, each of which has a standard deviation σ_i , then the standard deviation of R is provided by [23].

$$\sigma_R = \sqrt{\left(\frac{\partial R}{\partial \sigma_1}\right)^2 \sigma_1^2 + \left(\frac{\partial R}{\partial \sigma_2}\right)^2 \sigma_2^2 + \dots + \left(\frac{\partial R}{\partial \sigma_i}\right)^2 \sigma_i^2} \quad (1)$$

K-type thermocouple (made in China by UNI-T) width of 0.2 mm was used to check the water and tank walls'

temperatures. Temperature was recorded using 12 channels Model BTM-4208SD (Lutron Electronic Enterprise Co., LTD, Taiwan). BTM-4208SD is a paperless, real-time, 12-channel temperature recorder that uses SD cards to store data and time. Data can be measured and downloaded to Excel without additional software by recording year, month, day, minute, and second on the SD memory card. The K-type thermocouple and BTM-4208SD data logger were calibrated by Quality Measurement and Control Center in Iraq.

Table 1 provides a summary of the uncertainties that are associated with all experimental measuring devices. For each and every one of the examples, the highest amount of uncertainty in this study was 4%.

Table 1. The equipment used with its precision and lack of certainty

Equipment	Measurement Section	Accuracy	Uncertainty
K-type thermocouple	Temperature of water and surfaces	$\pm 0.5^{\circ}\text{C}$	0.15°C
BTM-4208SD data logger	Temperature recorder	$0.4\% + 0.5^{\circ}\text{C}$	0.3°C

3. EXPERIMENTAL APPARATUS AND PROCEDURE

Two horizontal water tanks made of polyethylene material with a capacity of 500 liters were used in a series of experiments that were carried out over the summer and winter seasons. Additionally, other tanks with a capacity of 1000 liters were used to surround one of the tanks in order to create an air gap of (20 mm). The Research Station of Mechanical Engineering at Kerbala University in Iraq (with a latitude angle of 32.6 degrees North, a longitude angle of 44.03 degrees East, and a mean altitude above sea level of 30 meters) was the location where these water tanks were tested and examined during the months of September and February of 2024. The first thing that needs to be done is to prepare the large tank by cutting off the top of it. After that, place one of the tanks inside it to make the air gap, as shown in Figure 1. After applying sealant material to prevent any leaks that were discovered in order to guarantee that the air gap would be closed, the chassis was ultimately subjected to a comprehensive inspection to check for any air leaks, particularly in the areas surrounding the edges and screw holes, as seen in Figure 2. As part of the experimental tests, the temperature is measured using ten thermocouples in each of

the two tanks. Eight of the thermocouples are located inside the tanks at various positions, while the other two thermocouples are located on the surfaces of the tanks, as shown in Figure 3.

The first step was to calibrate the thermocouples and data logger that would be used in the tests. The two tanks were also put in the same place so that they would have the same weather, as shown in Figure 2. After that, the same amount of water was put into both tanks. Finally, every hour the temperatures of the water at different depths inside the tanks and on the sides of the tanks were written down (Figure 3).



Figure 1. Prepare the large tank with one of the tanks to create the air gap



Figure 2. Experimental rig (the left tank without air gap and the right tank with air gap)

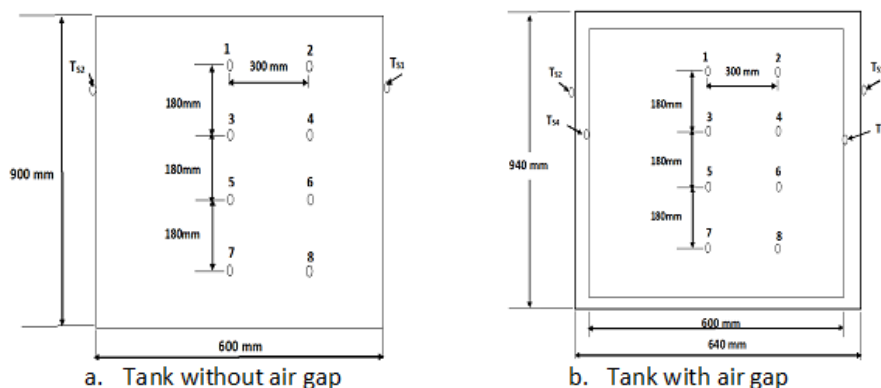


Figure 3. Thermocouple's locations in the tanks

4. NUMERICAL MODEL

Each of the cylindrical water tanks holds 500 litres, and one of them has an air pocket. The water tanks' schematic model is shown in Figure 4. Ansys Workbench software is used to build the geometry for the numerical simulation, and the Fluent platform is used to solve and post-process the solid and fluid domains. The boundary effects at the end walls in the z-direction are presumed to be insignificant, hence, a 2D model is employed in the simulations. Conduction is the sole mechanism of heat transfer in the aquatic environment, with all thermophysical properties of both water and tank material being constant and irrespective of temperature.

Table 2 lists the properties of the materials used for water tanks, as well as those of water and air. Since the water tanks are exposed to the atmosphere, conditions for convection and solar radiation are established for the tank's exterior. The quantity that reflects the combined effect of convection and solar radiation is known as a convective boundary.

This quantity is denoted by the symbol T_{solair} and is determined by applying Eq. (2) to the data for the months of September and January in the year 2024 at the location of Kerbala University in Iraq.

$$T_{solair} = T_a + \left(a * \frac{q}{h_o} \right) \quad (2)$$

where, q is the solar radiation, h_o is the convective heat transfer coefficient at the outer surface, T_a is the ambient temperature, and a is the absorptivity. 32°C is considered the water's initial temperature.

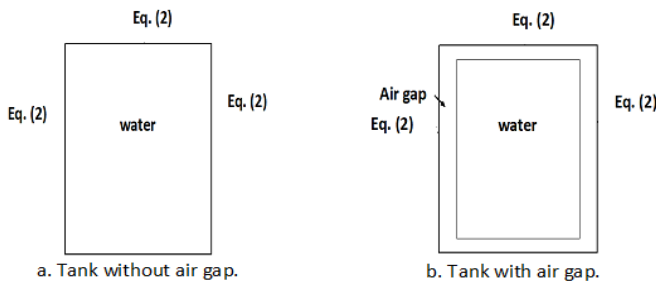


Figure 4. The geometry and boundary of the two water tanks

Table 2. Thermal properties of water tanks material

Material	Thermal Conductivity (W/m. °C)	Density (kg/m ³)	Specific Heat (kJ/kg.k)
Air	0.0242	1.225	1.006
Polycarbonate	0.39	950	2.3
Water	0.6	998.2	4.182

5. GOVERNING EQUATIONS

The following is an expression of the governing equations for this problem based on the previously discussed technique and the aforementioned assumptions:

$$\frac{\partial \rho}{\partial t} + \frac{\partial(\rho u)}{\partial x} + \frac{\partial(\rho v)}{\partial y} = 0 \quad (3)$$

$$\frac{\partial(\rho u)}{\partial t} + \frac{\partial(\rho u u)}{\partial x} + \frac{\partial(\rho u v)}{\partial y} = -\frac{\partial p}{\partial x} + \mu \left(\frac{\partial^2 u}{\partial x^2} + \frac{\partial^2 u}{\partial y^2} \right) \quad (4)$$

$$\frac{\partial(\rho v)}{\partial t} + \frac{\partial(\rho u v)}{\partial x} + \frac{\partial(\rho v v)}{\partial y} = -\frac{\partial p}{\partial y} + \mu \left(\frac{\partial^2 v}{\partial x^2} + \frac{\partial^2 v}{\partial y^2} \right) \quad (5)$$

$$C_p \left[\frac{\partial(\rho T)}{\partial t} + \frac{\partial(\rho u T)}{\partial x} + \frac{\partial(\rho v T)}{\partial y} \right] = k \left(\frac{\partial^2 T}{\partial x^2} + \frac{\partial^2 T}{\partial y^2} \right) \quad (6)$$

where, ρ is the density, u and v are the axial and vertical velocity components, p is the pressure, μ is the dynamic viscosity, c_p is the specific heat at constant pressure, and T is the temperature.

6. NUMERICAL PRODUCER

The commercial program ANSYS 16 was used to build the integrated system. The SIMPLEC algorithm and the second order upwind strategy were used to solve the governing equations described above. The calculation was considered to have found numerical convergence and the iteration was terminated when the residual sums of the momentum, energy, and continuity equations were all less than 10^{-12} . Pressure has an under-relaxation factor of 0.3, momentum of 0.7, and energy of 1. The results' independence from the mesh size and time step was established after extensive investigation.

7. VALIDATION OF SIMULATION MODEL

The numerical simulation of the tank without an air gap is evaluated against simulation findings for a concrete tank [18] from September, demonstrating strong concordance as illustrated in Figure 5. The simulation of the tank, both with and without an air gap, was compared to the experimental results for both conditions. The numerically simulated temperature profiles along the tanks exhibit strong concordance with the reported experimental findings, as illustrated in Figure 6.

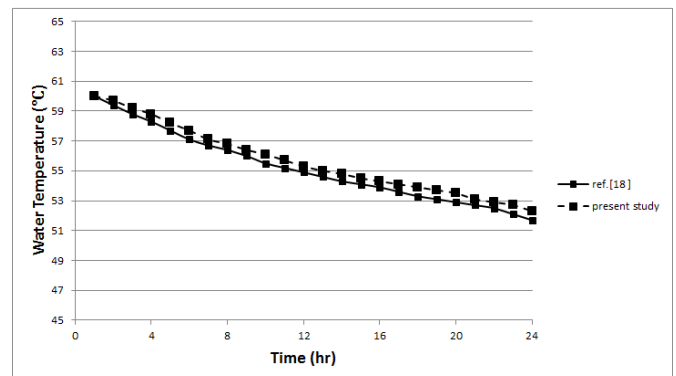
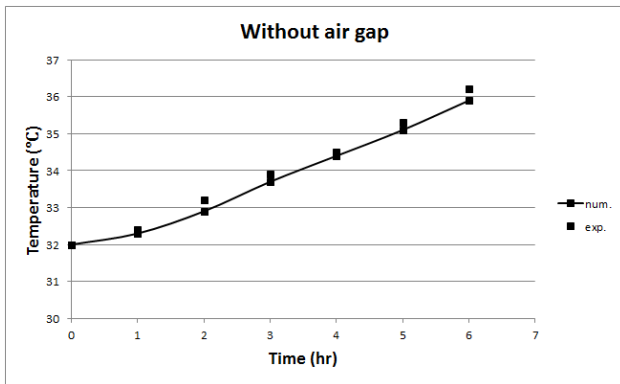
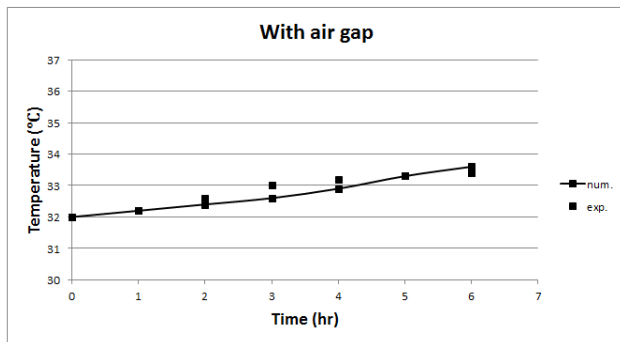


Figure 5. Validation of the numerical simulation carried out with reference [18]



(a) Without air gap



(b) With air gap

Figure 6. Comparison of the temperature of the experimental and numerical data over time

8. RESULTS AND DISCUSSION

This study examines the tanks in Kerbala city for the months of September, October, January, and February 2024, throughout a six-hour period from 8:00 AM to 2:00 PM. Figure 7 shows the air temperature during the day for Kerbala climate. Figure 8 displays the surface temperatures of the two tanks, both with and without an air gap, for the month of September (summer). The figure indicates that the influence of the air gap was initially negligible, becoming distinctly apparent after sunrise and persisting until dusk.

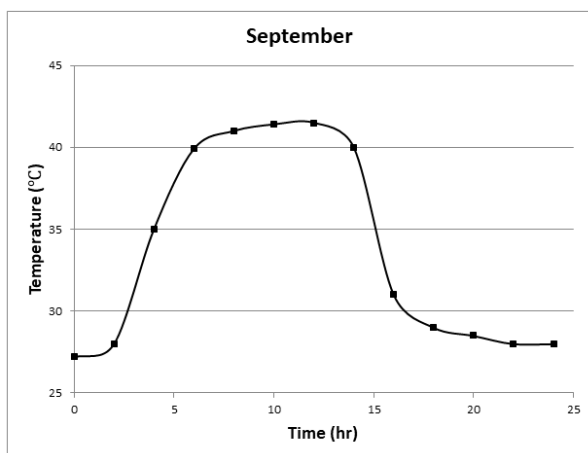


Figure 7. Air temperature during one day in September

Figures 9 and 10 illustrate the average water temperature for the two tanks, both numerically and experimentally, in September and January, respectively. It is evident that during

summer, the water temperature with an air gap is lower than that without an air gap, whereas in winter, the water temperature with an air gap is higher than that without an air gap. During the summer, the air gap reduces the amount of heat that is transferred from the environment to the water, and during the winter, it reduces the amount of heat that is transferred from the water to the environment.

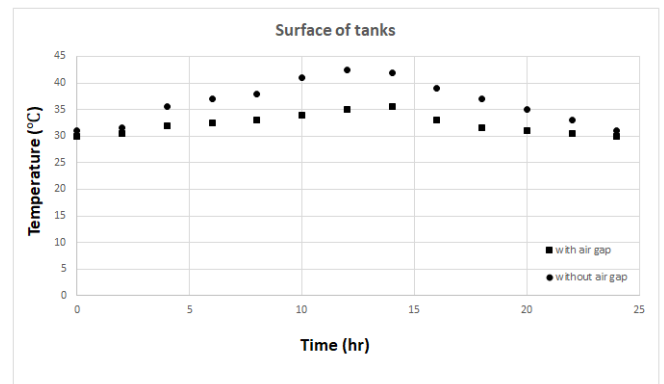
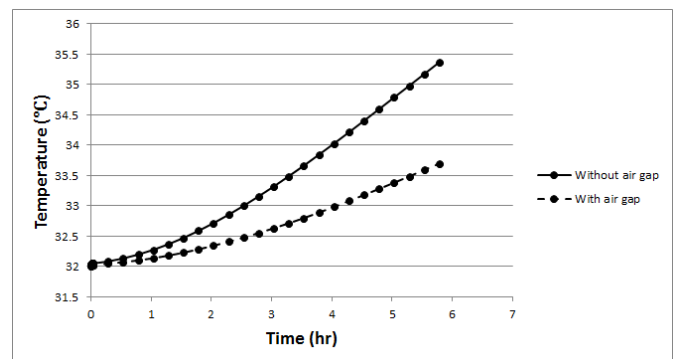
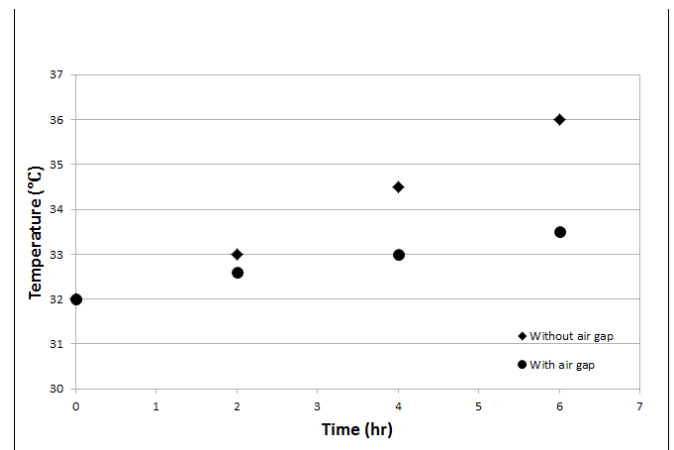


Figure 8. Surface temperature during the day



(a) Numerical

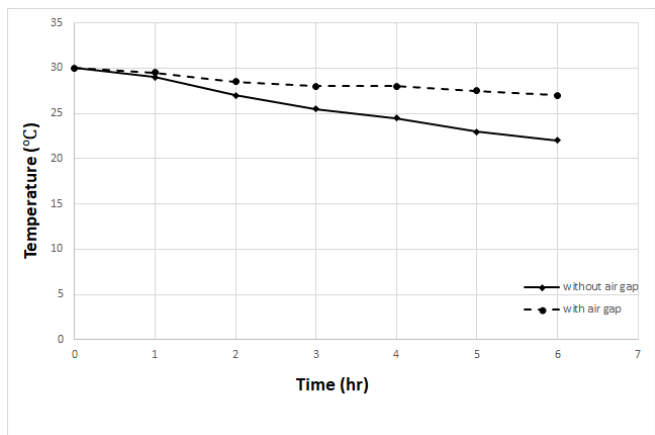


(b) Experimental

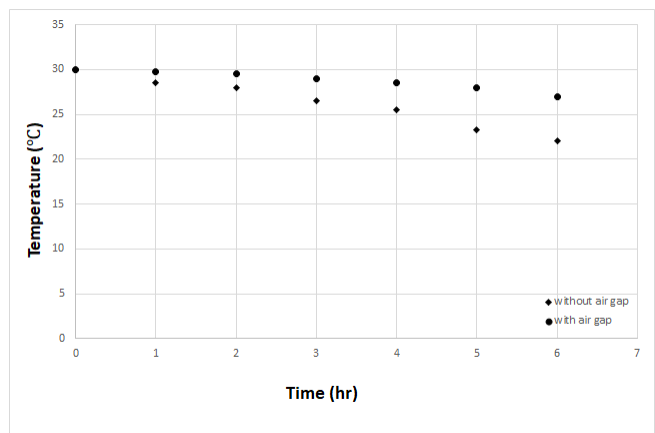
Figure 9. Comparison between average temperature of the two tanks: (a) numerically and (b) experimentally

Figures 11 and 12 displays the temperature ranges of the tanks from 8 a.m. to 2 p.m. in the summer and winter, with the right half having an air gap and the left half not having an air gap. From the shape, it's easy to see that the surface temperature of the tanks rises over time. The higher temperature near the surfaces is caused by a mix of convection, radiation, and transfer between the water and the tank wall.

After one hour, the temperature of the tank with the air gap was lower than the temperature of the tank without the air gap. This was true for all tests in the summer and higher in the winter.



(a) Numerical



(b) Experimental

Figure 10. Comparison between average temperature of the two tanks: (a) numerically and (b) experimentally

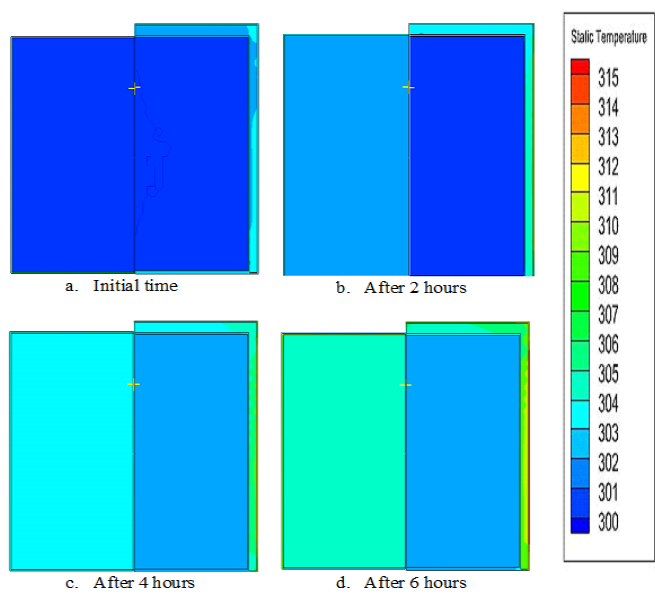


Figure 11. Temperature contour for the two tanks the left half without air gap and the right half with air gap for September

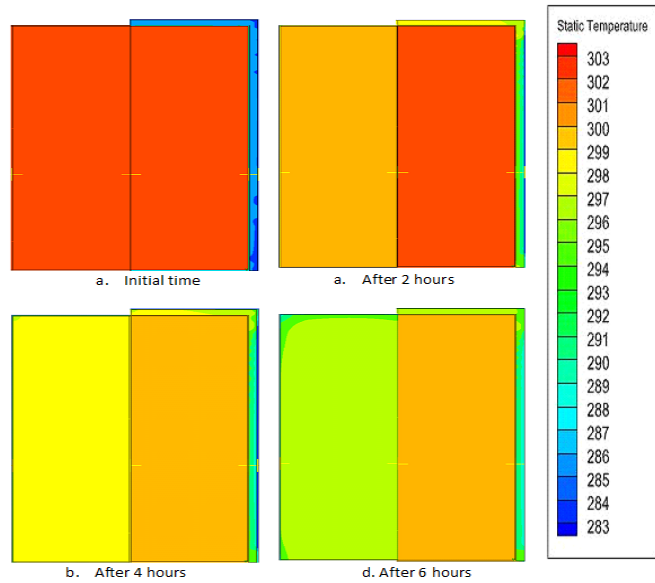


Figure 12. Temperature contour for the two tanks the left half without air gap and the right half with air gap for January

9. CONCLUSION

Keeping water storage tanks as efficient as possible requires minimising heat losses. The improvement of insulation equity, however, is often overlooked and so lacks any investigation in the literature. Reducing heat losses using traditional, highly thermally conductive materials could lead to larger storage systems, which would have an indirect effect on the cost of the storage. A technique that has been proposed to drastically reduce heat losses in water tanks is the use of air gap insulation. The purpose of this research was to determine how well a 500-liter water tank with an air gap performed in heat loss experiments meant for use in residential construction. During the summer and winter, two separate tests were carried out, one with and one without air gap tanks. The findings indicated that air gap insulation can significantly diminish heat loss in small residential water tanks.

REFERENCES

- [1] Acaravci, A., Ozturk, I. (2010). On the relationship between energy consumption, CO₂ emissions and economic growth in Europe. *Energy*, 35: 5412-5420. <https://doi.org/10.1016/j.energy.2010.07.009>
- [2] Palmer, J., Cooper, I., Cheng, V., et al. (2011). Great Britain's housing energy fact file, 2011. The Report, Department of Energy and Climate Change, UK. <https://www.gov.uk/government/publications/great-britains-housing-energy-fact-file-2011-excel-version>.
- [3] Van Blommestein, K.C., Daim, T.U. (2013). Residential energy efficient device adoption in South Africa. *Sustainable Energy Technologies and Assessments*, 1: 13-27. <https://doi.org/10.1016/j.seta.2012.12.001>
- [4] Rodriguez, I., Castro, J., Pérez-Segarra, C.D., Oliva, A. (2009). Unsteady numerical simulation of the cooling process of vertical storage tanks under laminar natural convection. *International Journal of Thermal Sciences*, 48(4): 708-721.

- <https://doi.org/10.1016/j.ijthermalsci.2008.06.002>
- [5] Fan, J., Furbo, S. (2012). Thermal stratification in a hot water tank established by heat loss from the tank. *Solar Energy*, 86(11): 3460-3469. <https://doi.org/10.1016/j.solener.2012.07.026>
- [6] Oliveski, R.D.C. (2013). Correlation for the cooling process of vertical storage tanks under natural convection for high Prandtl number. *International Journal of Heat and Mass Transfer*, 57(1): 292-298. <https://doi.org/10.1016/j.ijheatmasstransfer.2012.10.038>
- [7] Armstrong, P., Ager, D., Thompson, I., McCulloch, M. (2014). Improving the energy storage capability of hot water tanks through wall material specification. *Energy*, 78: 128-140. <https://doi.org/10.1016/j.energy.2014.09.061>
- [8] Padovan, R., Manzan M., De Zorzi E.Z., Gulli G., Frazzica A. (2015). Model development and validation for a tank in tank water thermal storage for domestic application. *Energy Procedia*, 81: 74-81. <https://doi.org/10.1016/j.egypro.2015.12.061>
- [9] Yang, Z., Chen, H.S., Wang, L., Sheng, Y., Wang, Y.F. (2016). Comparative study of the influences of different water tank shapes on thermal energy storage capacity and thermal stratification. *Renewable Energy*, 85: 31-44. <https://doi.org/10.1016/j.renene.2015.06.016>
- [10] Avignon, K., Kummert M. (2016). Experimental assessment of a phase change material storage tank. *Applied Thermal Engineering*, 99: 880-891. <https://doi.org/10.1016/j.applthermaleng.2016.01.083>
- [11] Cruickshank, C.A., Harrison, S.J. (2010). Heat loss characteristics for a typical solar domestic hot water storage. *Energy Build*, 42(10): 1703-1710. <https://doi.org/10.1016/j.enbuild.2010.04.013>
- [12] Abdelhak, A., Mhiri, H., Bournot, P. (2015). CFD analysis of thermal stratification in domestic hot water storage tank during dynamic mode. *Building Simulation*, 8: 421-429. <https://doi.org/10.1007/s12273-015-0216-9>
- [13] Rahman, A., Amanda, D., Nelson, F. (2016). Performance modeling and parametric study of a stratified water thermal storage tank. *Applied Thermal Engineering*, 100: 668-679. <https://doi.org/10.1016/j.applthermaleng.2016.01.163>
- [14] Erdemir, D., Atesoglu, H., Altuntop, N. (2019). Experimental investigation on enhancement of thermal performance with obstacle placing in the horizontal hot water tank used in solar domestic hot water system. *Renewable Energy*, 138: 187-197. <https://doi.org/10.1016/j.renene.2019.01.075>
- [15] Kursun, B. (2018). Thermal stratification enhancement in cylindrical and rectangular hot water tanks with truncated cone and pyramid shaped insulation geometry. *Solar Energy*, 169: 512-525. <https://doi.org/10.1016/j.solener.2018.05.019>
- [16] Kursun, B., Okten, K. (2018). Effect of rectangular hot water tank position and aspect ratio on thermal stratification enhancement. *Renewable Energy*, 116: 639-646. <https://doi.org/10.1016/j.renene.2017.10.013>
- [17] Bouzaher, M.T., Bouchahm, N., Guerira, B., Bensaci, C., Lebbi, M. (2019). On the thermal stratification inside a spherical water storage tank during dynamic mode. *Applied Thermal Engineering*, 159: 113821. <https://doi.org/10.1016/j.applthermaleng.2019.113821>
- [18] Bai, Y.L., Yang, M., Fan, J.H., Li, X.X., Chen, L.F., Yuan, G.F., Wang, Z.F. (2020). Influence of geometry on the thermal performance of water pit seasonal heat storages for solar district heating. *Building Simulation*, 14: 579-599. <https://doi.org/10.1007/s12273-020-0671-9>
- [19] Janakarajan, R., Prakash, D., Sundar, S., Kasthurirangan, L. (2018). Analysis and optimization of an insulated water for the domestic purpose. *Australian Journal of Mechanical Engineering*, 17(1): 1-10. <https://doi.org/10.1080/14484846.2018.1461732>
- [20] Khoury, S., Maatouk, C., El Khoury, K., Khatounian, F. (2022). Optimization methodology of thermal energy storage systems for domestic water heating applications with different configurations. *Journal of Energy Storage*, 50: 104530. <https://doi.org/10.1016/j.est.2022.104530>
- [21] Hwang, J., Kim, Y., Park, J., Rie, D. (2024). A study on the evaluation of thermal insulation performance of cellulose-based silica aerogel composite building materials. *Polymers*, 16(13): 1848. <https://doi.org/10.3390/polym16131848>
- [22] Liu, D.X., Zhang, W., Gu, D., Sun, T.Y. (2024). Experimental study on a new type of water storage tank for geothermal heating. *Geothermic*, 118: 102818. <https://doi.org/10.1016/j.geothermics.2024.102918>
- [23] Moffat, R. (1988). Describing the uncertainty in experimental results. *Experimental Thermal and Fluid Science*, 1(1): 3-17. [https://doi.org/10.1016/0894-1777\(88\)90043-X](https://doi.org/10.1016/0894-1777(88)90043-X)

NOMENCLATURE

a	absorptivity
C _p	Specific heat
h _o	Convective heat transfer coefficient
K	thermal conductivity
P	Pressure
q	Solar radiation
T	Temperature
t	time
u	Axial velocity
v	Vertical velocity

Greek letters

μ	dynamic viscosity
ρ	density
σ	standard deviation